International Journal of Fluid Power 3 (2002) No.3 pp. 13-18

AN EMPIRICAL DISCHARGE COEFFICIENT MODEL FOR ORIFICE FLOW

Duqiang Wu, Richard Burton and Greg Schoenau

Department of Mechanical Engineering, University of Saskatchewan, 57 Campus Drive, Saskatoon, Saskatchewan, Canada, S7N 5A9
duw612@mail.usask.ca

Abstract

In fluid power systems, flow control is mainly achieved by throttling the flow across valve orifices. Lumped parameter models are generally used to model the flow in these systems. The basic orifice flow equation, derived from Bernoulli's equation of flow, is proportional to the orifice sectional area and the square root of the pressure drop and is used to model the orifice coefficient of proportionality. The discharge coefficient, C_d, is often modeled as being constant in value, independent of Reynolds number.

However, for very small orifice openings, C_d varies significantly and can result in substantial error if assumed constant. In this situation, modelers usually revert to graphs or look–up tables to determine C_d. This paper provides a closed form model for C_d as a function of the Reynolds number which can be applied to different types of orifices. Based on this model, a technique to evaluate flow given an orifice area and pressure drop without having to use iteration is introduced.

Keywords: fluid power, hydraulic, flow control, orifice equation, discharge coefficient, Reynolds number

1 Introduction

The well known equation of the volumetric flow rate through an orifice (Fig. 1) is derived from Bernoulli's equation by assuming (1) an incompressible fluid and (2) turbulent flow as

$$Q = C_d A \sqrt{\frac{2}{\rho}\left(P_u - P_{vc}\right)} \tag{1}$$

where

$$C_d = \frac{C_v C_c}{\sqrt{1 - C_c^2\left(A/A_u\right)^2}} \tag{2}$$

C_v, flow velocity coefficient (approximately 0.98).
C_c, area contraction coefficient (equal to A_{vc}/A).
For sharp-edged orifices, it is 0.611.
A_{vc}, the cross-sectional area at *vena contracta*.
A_u, the cross-sectional area at upstream.
P_u, the pressure at upstream.
P_{vc}, the pressure at vena contracta.

Because A_u is much larger than A, the discharge coefficient, C_d, is almost equal to $C_v C_c$.

This manuscript was received on 12 September 2002 and was accepted after revision for publication on 02 December 2002

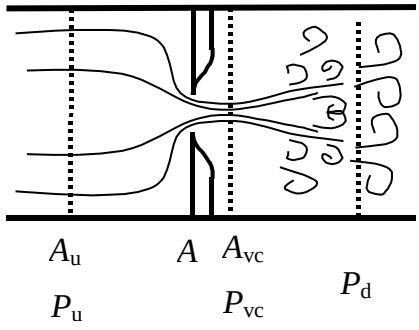

Fig. 1: *Flow through a sharp-edged orifice*

Because in many situations, the flow through an orifice is turbulent, the discharge coefficient, C_d, is commonly considered as a constant. Application of Eq. 1 can also be extended to the case of laminar flow. In this case, the discharge coefficient is a function of the Reynolds number as well as the orifice geometry and is usually determined by experimental methods and presented graphically (Merritt, 1967). Viall et al (2000) experimentally determined the discharge coefficient of a typical spool valve. Borghi et al (1998) and Vescovo et al (2002) employed computational fluid dynamics (CFD) models to numerically compute the discharge coefficient and compared the computational and experimental results. None of these studies or other CFD studies (Ellman et al, 1996; Gromala et al, 2002), etc.

developed a functional relationship between the discharge coefficient and Reynolds number. A main reason is that the Reynolds number also depends on the flow rate requiring an iterative numerical solution (Miller, 1996).

This paper provides an empirical model of the discharge coefficient with respect to square root of Reynolds number. This empirical model can be directly applied to traditional graphically-expressed functions, $C_d = f\left(\sqrt{Re}\right)$, for sharp-edged orifices (such as that provided by Merritt (1967)), or to experimentally derived discharge coefficients (such as that provided in this paper). The paper will also consider the determination of parameters in the generalized empirical model for an orifice. Finally, a new calculation method for the flow rate, which does not need iteration, with the empirical model is developed.

2 Empirical Modelling of Discharge Coefficient for Orifices

From the literature, it is well known that there is a transition in a plot of discharge coefficient vs. $\sqrt{Re}$ from being proportional to the square root of the Reynolds number, *Re*, at low Reynolds number, to being constant at high *Re*. Although the curve shapes vary as the orifice geometry varies, they can be approximated by an empirical model as an exponential function, i.e:

$$C_d = C_{d\infty}\left(1 - e^{-\frac{\delta}{C_{d\infty}}\sqrt{Re}}\right) \tag{3}$$

where $C_{d\infty}$ is the turbulent discharge coefficient for a specific orifice. δ is a laminar discharge coefficient, and is similar to the coefficient introduced graphically by Merritt (1967).

Equation 3 is simple and the two parameters have a clear physical interpretation. $C_{d\infty}$ is the turbulent discharge coefficient because C_d converges to $C_{d\infty}$ for high Reynolds numbers. δ is called as "laminar discharge coefficient" because Eq. 3 can be approximated by $C_d = \delta\sqrt{Re}$ at very small Reynolds numbers $\left(\left.\frac{\partial C_d}{\partial\sqrt{Re}}\right|_{\sqrt{Re}=0} = \delta\right)$.

However, Eq. 3 cannot always be satisfied for a variety of orifices with different geometries, especially when fitting the transition from the laminar flow to turbulent flow.

Therefore, another form of the discharge coefficient is proposed as

$$C_d = C_{d\infty}\left(1 + ae^{-\frac{\delta_1}{C_{d\infty}}\sqrt{Re}} + be^{-\frac{\delta_2}{C_{d\infty}}\sqrt{Re}}\right) \tag{4}$$

where the parameters, *a*, *b*, δ_1 and δ_2 are specific flow dependent coefficients to be determined. Equation 4 can be applied to most types of orifice.

Three types of orifices with the different geometries shown in Fig. 2 are modeled using the generalized empirical model (Eq. 4). The sharp-edged orifice (Fig. 2(a)) has zero length and near 180° trumpet mouth downstream. The spool orifice (Fig. 2(b)) has a 90° downstream mouth. The needle orifice (Fig. 2(c)) has a downstream mouth less than 90°. The shape of discharge coefficient curves for each would be different and it is now necessary to consider the application of the empirical model (Eq. 4) to these typical orifices.

(a) Sharp-edged Orifice (b) Sharp-edged pool orifice (c) Needle valve orifice

Fig. 2: *Three types of orifice*

2.1 Application of the empirical model to typical curve of discharge coefficient

Merritt (1967) has presented a "smooth" discharge coefficient curve with respect to square root of Reynolds number for a typical sharp-edged orifice (Fig. 2(a)). This smooth curve has been generated from experimental data. For this curve, the parameters, *a*, *b*, δ_1 and δ_2 in Eq. 4 can be determined using the following mathematical manipulation. The laminar discharge coefficient, δ, the turbulent discharge coefficient, $C_{d\infty}$, and the maximum discharge coefficient, C_{dm}, at a specific Reynolds number, Re_m, can be found by applying an appropriate measurement on a given curve. The four parameters, *a*, *b*, δ_1 and δ_2 can be solved by applying the following four conditions common to most types of orifices:

1. Initial condition:

$$C_d\big|_{\sqrt{Re}=0} = 1 + a + b = 0 \tag{5}$$

2. Laminar discharge coefficient condition:

$$\left.\frac{\partial C_d}{\partial\sqrt{Re}}\right|_{\sqrt{Re}=0} = -a\delta_1 - b\delta_2 = \delta \tag{6}$$

For a sharp edged orifice, $\delta \approx 0.2$.

3. Maximum value conditions:

$$C_{dm} = C_{d\infty}\left(1 + ae^{-\frac{\delta_1}{C_{d\infty}}\sqrt{Re_m}} + be^{-\frac{\delta_2}{C_{d\infty}}\sqrt{Re_m}}\right) \tag{7}$$

and

$$\left.\frac{\partial C_d}{\partial\sqrt{Re}}\right|_{\sqrt{Re_m}} = -a\delta_1 e^{-\frac{\delta_1}{C_{d\infty}}\sqrt{Re_m}} - b\delta_2 e^{-\frac{\delta_2}{C_{d\infty}}\sqrt{Re_m}} = 0 \tag{8}$$

Equation 5 through 8 can be solved to determine *a*, *b*, δ_1 and δ_2. These equations can be simplified into a non-linear algebraic equation of δ_1 as

$$\delta_1 = \frac{\delta e^{-\frac{\delta_2}{C_{d\infty}}\sqrt{Re_m}}}{\frac{C_{dm}}{C_{d\infty}} - 1 + e^{-\frac{\delta_2}{C_{d\infty}}\sqrt{Re_m}}} \quad (9)$$

where

$$\delta_2 = \frac{\delta e^{-\frac{\delta_1}{C_{d\infty}}\sqrt{Re_m}}}{\frac{C_{dm}}{C_{d\infty}} - 1 + e^{-\frac{\delta_1}{C_{d\infty}}\sqrt{Re_m}}} \quad (10)$$

Equation 9 and 10 can be solved numerically. Parameters, *a* and *b*, can be determined by

$$a = \frac{\delta - \delta_2}{\delta_2 - \delta_1} \quad (11)$$

$$b = \frac{\delta - \delta_1}{\delta_1 - \delta_2} \quad (12)$$

Note that a maximum value of discharge coefficient does not always exist in the transition region from the laminar to the turbulent flow. In this case, Re_m can be considered to be an intersecting point of two asymptote lines for the laminar and turbulent flow regions. Thus, the right hand side of Eq. 8 would not be zero, but some finite value, $\dot{C}_{dm}$. Equation 9 and 10 then become

$$\delta_1 = \frac{\delta e^{-\frac{\delta_2}{C_{d\infty}}\sqrt{Re_m}} - \dot{C}_{dm}}{\frac{C_{dm}}{C_{d\infty}} - 1 + e^{-\frac{\delta_2}{C_{d\infty}}\sqrt{Re_m}}} \quad (13)$$

and

$$\delta_2 = \frac{\delta e^{-\frac{\delta_1}{C_{d\infty}}\sqrt{Re_m}} - \dot{C}_{dm}}{\frac{C_{dm}}{C_{d\infty}} - 1 + e^{-\frac{\delta_1}{C_{d\infty}}\sqrt{Re_m}}} \quad (14)$$

The method is applied to the typical discharge coefficient curve given by Merritt (1967) (pp. 44). The input and output parameters for the model calculations are listed in Table 1.

Table 1: Empirical model parameters for a typical coefficient curve

Input Parameters	$C_{d\infty}$	δ	C_{dm}	$\sqrt{Re_m}$
	0.61	0.23	0.69	11
Output Parameters	A	b	δ_1	δ_2
	1.07	-2.07	0.077	0.15

Using these parameters, the empirical model of the discharge coefficient for Merritt's curve becomes

$$C_d = 0.61\left(1 + 1.07e^{-0.126\sqrt{Re}} - 2.07e^{-0.246\sqrt{Re}}\right) \quad (15)$$

and is shown in Fig. 3. Excellent agreement between the original curve and the empirical model predictions is obtained.

2.2 Application of the empirical model to experimental data plot of discharge coefficient

Although Fig. 3 is a commonly used plot of discharge coefficient for a sharp-edged orifice, in practice, the clearance, chamfer, and other factors of valves (due to machining accuracy limitation) generate a different shaped curve. Thus, it is necessary to measure the discharge coefficient for the orifice of specific valves. The method of the experimental determination of the discharge coefficient, C_d, and the corresponding Reynolds number, *Re*, for an orifice are also based on the general flow equations:

$$C_d = \frac{Q}{A\sqrt{\frac{2}{\rho}\Delta P}} \quad (16)$$

$$Re = \frac{\rho\left(Q/A\right)D_h}{\mu} \quad (17)$$

where Q is the flow rate through the orifice, A is the cross-sectional area of the orifice, ΔP is the pressure drop cross the orifice, D_h is the hydraulic diameter, ρ is the fluid density and μ is the fluid absolute viscosity.

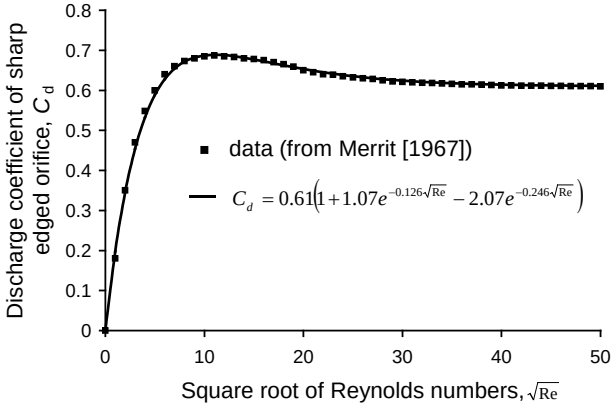

Fig. 3: *Comparison between typical discharge coefficient and the empirical model predictions*

The experimental hydraulic circuit was so designed such that the pressure differential, ΔP, of the tested orifice could be adjusted. In order to create a variety of flow conditions, each of the orifice opening, *x*, the fluid temperature, *T*, and the pressure differential, ΔP, was set at different levels to carry out the experiment. The purpose of varying the fluid temperature, *T*, was to change in a controlled form, the fluid absolute viscosity, μ. The three variables were selected so that the orifice flow condition could span the laminar, the transient and turbulent regions. For these different flow conditions through the orifice, Q, ΔP, x, and T, are measurable. A and D_h can be calculated from x, based on the orifice geometry. Consequently, the discharge coefficient, C_d, and the Reynolds number, *Re*, can be determined from Eq. 16 and 17.

Experimental results for the discharge coefficient for a specific sharp-edged spool orifice used in the study are given in Fig. 4. The data was obtained for the

fixed orifice of a PC valve manufactured by Brand Hydraulics Inc (model: EFC12-10-12).

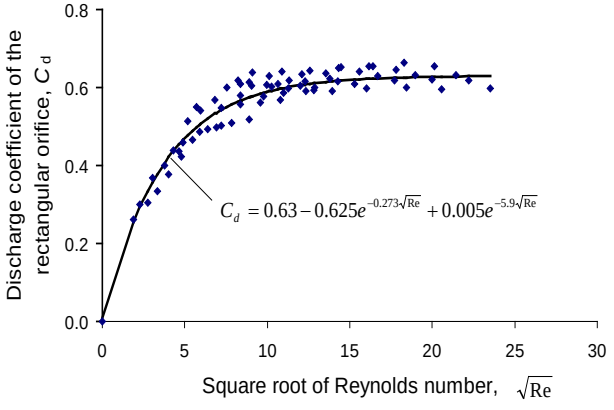

Fig. 4: *Comparison between the measured results and empirical model of the discharge coefficient for a typical sharp-edged spool orifice*

The discharge coefficient of a typical needle valve orifice was also experimentally determined (Fig. 5) for a ¾" needle valve manufactured by Deltrol Fluid Prod (Model: EN-35).

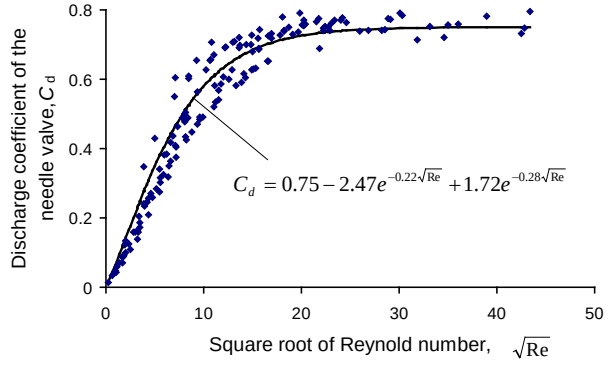

Fig. 5: *Comparison between the measured results and empirical model of the discharge coefficient for a typical needle valve orifice*

Consider the application of the empirical model to these two experimental results. It is noted that the mathematical method introduced in Section 2.1 cannot be applied to these experimental data because the input parameters, $C_{d\infty}$, δ, Re_m, C_{dm}, and $\dot{C}_{dm}$, cannot be accurately measured from the plot of the experimental data. Therefore, an alternate technical method is introduced to evaluate the various coefficients from experimental data with normal scatter.

This alternative method of obtaining model coefficients, $C_{d\infty}$, a, b, δ_1 and δ_2, is nothing more than the direct application of curve fitting. In this case, the typical parameters, $C_{d\infty}$, C_{dm}, δ, Re_m, and $\dot{C}_{dm}$ do not need to be known. The solution of $C_{d\infty}$, a, b, δ_1 and δ_2 should make the following objective function a minimum.

$$J = \sum_{i=1}^{N}\left[w_i \left(C_{di} - C_{d\infty}\left(1 + ae^{-\frac{\delta_1}{C_{d\infty}}\sqrt{Re_i}} + be^{-\frac{\delta_2}{C_{d\infty}}\sqrt{Re_i}} \right) \right) \right]^2 \quad (18)$$

where w_i is the weight coefficient at Re_i. C_{di} is the experimental discharge coefficient at the point Re_i. The optimal method of searching multi-parameters is suitable for solving $C_{d\infty}$, a, b, δ_1 and δ_2 from the direct experimental results. It must be recognized, however, that a significant amount of computation is necessary because the curve fit using Eq. 18 includes five unknown parameters. Models generated using the curve fitting method (as well as the predicted values) were also illustrated in Fig. 4 and 5.

3 Application in Fluid Power Simulations

In section 2 of this paper, a method has been presented for developing equations for directly calculating C_d as a function of Re from experimental data which has been smoothed or with experimental scatter. However, to make use of the curve for modelling purposes, iterative procedures must be used because the Reynolds number is a function of flow rate. This can be observed from the equation relating flow to pressure drop across an orifice obtained by substituting Eq. 4 into the general flow Eq. 1 which gives

$$Q = C_{d\infty}\left(1 + ae^{-\frac{\delta_1}{C_{d\infty}}\sqrt{Re}} + be^{-\frac{\delta_2}{C_{d\infty}}\sqrt{Re}} \right) A\sqrt{\frac{2}{\rho}\Delta P} \quad (19)$$

and the equation for Reynolds number expressed as a function of flow rate by

$$Re = \frac{\rho\left(Q/A\right)D_h}{\mu} \quad (20)$$

Consider a rectangular orifice of width, w, and opening of a small distance, x, where $w >> x$. Re can be expressed as

$$Re = \frac{2Q\rho}{w\mu} \quad (21)$$

Substituting Eq. 21 into Eq. 19 gives

$$Q = C_{d\infty}\left(1 + ae^{-\frac{\delta_1}{C_{d\infty}}\sqrt{\frac{2Q\rho}{w\mu}}} + be^{-\frac{\delta_2}{C_{d\infty}}\sqrt{\frac{2Q\rho}{w\mu}}} \right) wX \quad (22)$$

where

$$X = x\sqrt{\frac{2}{\rho}\Delta P} \quad (23)$$

An iterative solution to this equation is required for all combinations of the variable, X. This means that, for each time step in a simulation, a series of interactions must be implemented as follows. Given a specific value for X, the initial flow rate, Q_0, is calculated using the discharge coefficient for large Reynolds numbers, $C_{d\infty}$. This would be used to calculate an initial Reynolds

number, Re_0 which would be used to calculate a new C_d, and subsequently, a new Q. The process is repeated until the difference in calculated flow rate between iterations reaches some accepted value.

Alternatively, for a specific value of X, it is possible to solve for C_d "off line" before the simulation is in fact started. This requires that the converged value of C_d be plotted as a function of some convenient variable. In this work, the initial Reynolds number Re_0 is used. This essentially eliminates the need for time consuming iterative solutions during dynamic simulation. The process requires calculating Re_0 off line (from X), using iterations to find the converged value for C_d and then plotting C_d vs. $\sqrt{Re_0}$. To use this new plot, either a look-up table or a functional empirical relationship can be used.

To demonstrate this, the off line process was applied to the sharp-edged orifice of Merritt (1967). This is shown in Fig. 6. It is noted worthy that the shape of the curve is similar to the original C_d vs. $\sqrt{Re}$ curve. Thus Eq. 4 could be used to approximate the curve with reasonable accuracy.

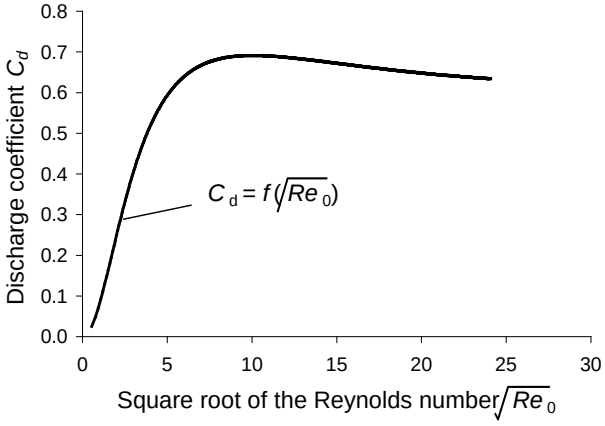

Fig. 6: *The modified discharge coefficient of the sharp-edged orifice*

4 Conclusions

This paper provides an empirical discharge coefficient model of flow rate through orifices. It can be applied to a variety of orifices with different geometries. Two approaches for solving the parameters in the empirical model are also developed. They can be applied to the "smooth" representations of the discharge coefficient and to experimentally determined C_d (with scatter) as a function of the Reynolds number. A simple method of using an off line value of C_d vs. the initial Reynolds numbers is introduced for use in modelling applications. This reduces the need for on line iterations. As a final note, the closed form of discharge coefficient as a function of Reynolds number makes it possible to mathematically manipulate the orifice flow rate equation, such as differentiating the flow rate to obtain the analytical expression of the flow gain, K_q, and pressure sensitivity, K_c. This is extremely important in determining stability criterion using small signal analysis of hydraulic systems at small orifice openings.

Nomenclature

A	orifice cross-sectional area	[m^2]
a, b	coefficients in the empirical model	[-]
A_u	flow cross-sectional area at upstream	[m^2]
A_{vc}	flow cross-sectional area at vena contracta [m^2]	
C_c	area contraction coefficient	[-]
C_d	discharge coefficient	
$C_{d\infty}$	turbulent discharge coefficient	
C_{dm}	maximum of discharge coefficient	
$\dot{C}_{dm}$	tangent of discharge coefficient at $\sqrt{Re_m}$	
C_v	velocity coefficient	[-]
D_h	hydraulic diameter	[m]
ΔP	pressure drop cross orifice	[Pa]
P_d	downstream pressure	[Pa]
P_u	upstream pressure	[Pa]
P_{vc}	pressure at vena contracta	[Pa]
Q	volumetric flow rate	[m^3/s]
Q_0	initial volumetric flow rate calculated from the turbulent discharge coefficient, C_d	[m^3/s]
Re	Reynolds number	[-]
Re_m	Reynolds number at maximum value or a specific point	[-]
Re	initial Reynolds number calculated from Q_0 associated with the turbulent discharge coefficient, $C_{d\infty}$.	[-]
S	orifice perimeter	[m]
w	rectangular orifice width	[m]
w_i	weight	[-]
X	variable associated with x, ΔP and ρ.	[-]
x	orifice opening	[m]
δ	laminar discharge coefficient	[-]
δ_1, δ_2	attenuation coefficients of the empirical model	[-]
μ	absolute viscosity	[Pas]
ρ	fluid density	[kg/m³]

Acknowledgements

The authors are grateful to visiting professor Jian Ruan from Zhejiang University of Technology of China and engineer Doug Bitner for their beneficial suggestions and help. This research was possible through the financial support of NSERC grants RGPIN 17061-99 and RGPIN 3689-00.

References

Borghi, M., Cantore, G., Milani, M. and **Paoluzzi, R.** 1998. Analysis of Hydraulic Components using Computational Fluid Dynamics Models. *Proceedings of the Institute of Mechanical Engineers*. V212 Part C. pp. 619.

Ellman, A. and Piche, R. 1996. A Modified Orifice Flow Formula for Numerical Simulation of Fluid Power Systems. *Fluid Power Systems and Technology, ASME*, Vol. 3, pp. 59-63.

Gromala, P., Domagal, M. and **Lisowski, E**. 2002. Research on Pressure Drop in Hydraulic Components by Means of CFD Method on Example of Control Valve. *Proceedings of the 2nd International FPNI PhD Symposium on Fluid Power*. Modena, Italy.

Merritt, H. E. 1967. *Hydraulic Control Systems.* John Wiley & Sons, Inc.

Miller, R. W. 1996. *Flow Measurement Engineering Handbook*, 3rd. McGraw-Hill, New York.

Vescovo, G. D. and **Lippolis, A.** 2002. Flow Forces Analysis on a Four-way Valve. *Proceedings of the 2nd International FPNI PhD Symposium on Fluid Power*. Modena, Italy.

Viall, E. and **Zhang, Q.** 2000. Spool Valve Discharge Coefficient Determination. *Proceedings of the 48th National Conference on Fluid Power*. Milwaukee, Wisconsin, USA. pp. 491.

Duqiang Wu
Graduate student for Ph.D. at present, Mechanical Engineering Department, University of Saskatchewan in Canada. Master (1984) at Nanjing University of science and Technology in China. Engineer (1986) at Shaanxi Mechanical and Electrical Institute in China. Visiting Scholar (1997) at University of Illinois at Urbana-Champaign.

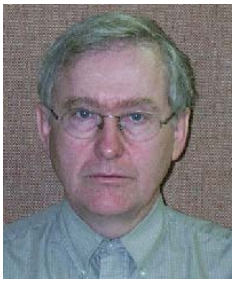

Richard Burton
P.Eng, Ph.D, Assistant Dean of the college of Engineering, Professor, Mechanical Engineering, University of Saskatchewan. Burton is involved in research pertaining to the application of intelligent theories to control and monitoring of hydraulics systems, component design, and system analysis. He is a member of the executive of ASME, FPST Division, a member of the hydraulics' advisory board of SAE and NCFP and a convenor for FPNI.

Greg Schoenau
Professor of Mechanical Engineering at the University of Saskatchewan. He was head of that Department from 1993 to 1999. He obtained B.Sc. and M. Sc. Degrees from the University of Saskatchewan in mechanical engineering in 1967 and 1969, respectively. In 1974 he obtained his Ph.D. from the University of New Hampshire in fluid power control systems. He continues to be active in research in this area and in the thermal systems area as well. He has also held positions in numerous outside engineering and technical organizations.